Repulsive Casimir forces between solid materials with high-refractive-index intervening liquids

P. J. van Zwol and G. Palasantzas

Department of Applied Physics, Materials Innovation Institute M2i and Zernike Institute for Advanced Materials,
University of Groningen, NL-9747 AG Groningen, The Netherlands

In order to explore repulsive Casimir or van der Waals forces between solid materials with liquid as the intervening medium, we analyze dielectric data for a wide range of materials as, for example, (p)olytetrafluoroethylene, polystyrene, silica, and more than 20 liquids. Although significant variation in the dielectric data from different sources exists, we provide a scheme based on measured static dielectric constants, refractive indices, and applying Kramers-Kronig consistency to dielectric data to create accurate dielectric functions at imaginary frequencies. The latter is necessary for more accurate force calculations via the Lifshitz theory, thereby allowing reliable predictions of repulsive Casimir forces.

I. INTRODUCTION

Repulsive Casimir forces between two surfaces can be of high technological interest in low-friction devices [1–4]. Measured repulsive Casimir forces have only been reported in a handful of papers [1–4]. As a matter of fact, repulsive Casimir forces between solids arise when the dielectric functions ε of material surfaces 1 and 2 and an intervening liquid obey the relation $\varepsilon_1(i\zeta) > \varepsilon_{\text{liquid}}(i\zeta) > \varepsilon_2(i\zeta)$ over a wide frequency range ζ. In most reports so far, one of the surfaces is a metal, the other a low-index material such as Teflon or silica, with an intervening nonpolar liquid having a relatively high refractive index.

The major difficulty for predicting repulsive Casimir forces in liquids is that the calculated force itself is rather uncertain [5,6]. This is because the dielectric function of most liquids in force calculations is not very different from the low-index materials used in experimental systems [1–4]. Small variation in the dielectric data due to sample dependence or measurement uncertainty can easily lead to forces of opposite sign for one set of dielectric data compared to another for the same system. Contrary to solid materials, for very pure liquids we would not expect sample dependence of the dielectric function. This is because neither grains nor defects exist in a liquid, nor does the density vary significantly at atmospheric conditions. Therefore, it is relatively surprising that variations in dielectric data for liquids are often reported in the literature [6].

Furthermore, the more serious problem for all studies reported on repulsive Casimir forces is that the corresponding theory calculations were based on simple oscillator models, which were built from limited dielectric data (see [7] for the construction of oscillator models). Theoretical force predictions based on these models can easily be incorrect by an order of magnitude. Therefore, oscillator models are not suitable for accurate force calculations in solid-liquid systems [6]. On the other hand, oscillator models were developed because precise knowledge of the VUV (vacuum ultraviolet) dielectric data for most substances was not available [7]. It is only in the last two decades that many dielectric data have become available, however, with large reported variation [6].

In order to overcome the problem of varying dielectric data in liquids and to improve the force calculations in

terms of Lifshitz theory, we present a method to handle measured dielectric data that is based on the Kramers-Kronig (KK) consistency of measured refractive index (n), extinction coefficient (k), or measured dielectric absorption, and the static dielectric constant ε_0. All dielectric data used here cover the major IR (infrared) and UV ranges, providing therefore a reliable base for more accurate force calculations than in the past. Before proceeding, we wish to point out that in essence, we combine the method behind the construction of oscillator models described in Ref. [7] (for which the major concern is the determination of the fundamental frequencies of the oscillators) with frequency-dependent dielectric data covering all the fundamental absorption frequencies.

II. DIELECTRIC DATA ANALYSIS: APPLICATION TO TEFLON

Polytetrafluoroethylene (PTFE or Teflon) is possibly the best known material for which Casimir repulsion was found [1–3]. However, the corresponding force measurements with this substance were compared to theory, which was based on simple second-order oscillator models, since the complete dielectric function of PTFE was simply unknown. Here we were able to construct the dielectric function of PTFE from recent literature data (see Appendix) [8–11] as Fig. 1 shows.

The VUV data give the most important contribution to the dielectric function $\varepsilon(i\zeta)$ at imaginary frequencies, as shown in Fig. 1(a). But, we have used only a molecule [poly(hexafluoro-1,3-butadiene) or PHFBD] similar to PTFE to obtain the dielectric function in this range because no other data were available. In general, all fluoropolymers have very similar dielectric responses, with a first absorption peak at $\sim 8\,\text{eV}$ and a second one at $\sim 20\,\text{eV}$. In order to confirm the validity of using the PHFBD data, further tests are necessary. For this purpose, we use the KK transform

$$n(i\zeta) = 1 + \frac{2}{\pi} \int_0^{+\infty} \frac{\omega\, k(\omega)}{\omega^2 + \zeta^2} d\omega, \tag{1}$$

with $\varepsilon(i\zeta) = n(i\zeta)^2$ the dielectric function at imaginary frequencies. The latter is important for force calculations in terms of the Lifshitz theory. If the KK transform is applied over
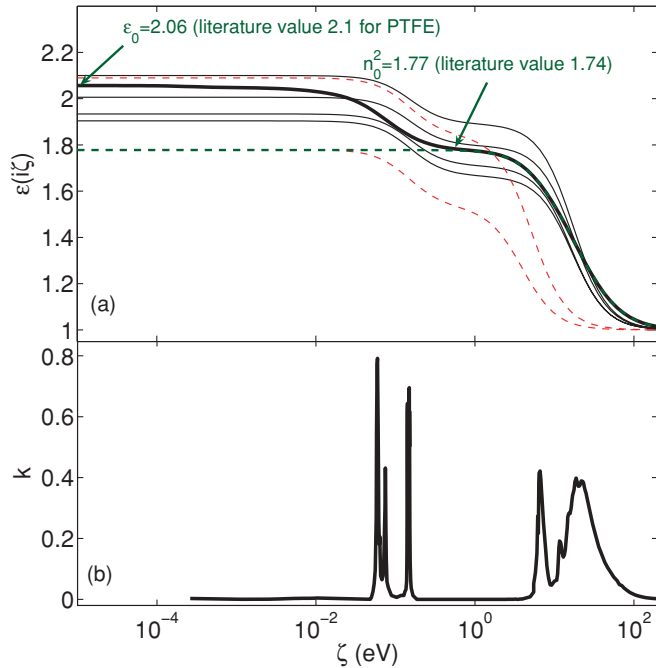
FIG. 1. (Color online) (a) Dielectric function at imaginary frequencies for PTFE. The thick black line is from data as described in text. Thin lines are oscillator models for low- and high-density Teflon derivatives [12]. Red dashed lines are oscillator models from Ref. [1]. The n_0^2 plateau is also shown (horizontal green) dashed line. (b) Raw dielectric data for PTFE.

all relevant frequency ranges, then for $\zeta = 0$ the function $\varepsilon(i\zeta)$ should reproduce the dielectric constant ε_0 [7]. In addition, when a substance is transparent in the near-IR and visible range [existence of well-defined plateau in the $\varepsilon(i\zeta)$ vs ζ plot; see Fig. 1], the KK transform over the UV and x-ray frequency range yields for $\zeta = 0$ the squared refractive index n_0^2 in the visible range (e.g., at the wavelength $\lambda = 589.3$ nm). When IR absorption is negligible, then $n_0^2 \approx \varepsilon_0$ holds [7]. The substances discussed in this work are all transparent in the near-IR, visible, and near-UV ranges. In addition, data for ε_0 and n_0 are known accurately (within a few percent accuracy) for almost any substance. Therefore we are demanding that the less precise experimental data in the VUV regime are corrected in order to be KK consistent with the more accurate refractive index n_0 in the visible range or with the dielectric constant ε_0 (if some IR absorption is present as in the case of PTFE; Fig. 1).

Although the choice of the wavelength $\lambda = 589.3$ nm in the visible range where we obtain the value of n_0 might seem rather arbitrary, for most transparent substances it is located in the regime between the major IR and UV absorption peaks, where also the value of $n(\omega)$ varies the least [well-defined plateau in $\varepsilon(i\zeta)$ vs ζ; Fig. 1(a).] Moreover, n_0^2 ($\lambda = 589.3$ nm) is well measured and documented in the literature for almost any substance. For example, for water, n_0 varies from 1.32 to 1.34 for the wavelength range 1300–500 nm. The fact that $n_0^2(589.3 \text{ nm}) \approx \varepsilon_0$ within 1% for all nonpolar liquids with little IR absorption reflects this consideration (see also Table I). Note at last that for the alkanes with negligible IR absorption (Table I), the value of n_0^2 (589.3 nm) agrees quite well (to within 2%) with the reported strength of ε_0 and n_0 where

Cauchy plots were used to determine n_0 [7]. In contrast to liquids with negligible IR absorption, for PTFE the value of n_0^2 (589.3 nm) differs from ε_0 by $\sim$15% due to two major peaks in the IR range (Fig. 1).

Thus, the dielectric function at imaginary frequencies should reproduce the ε_0 and n_0^2 values. If the measured data for the extinction coefficient k or the absorptive part of the dielectric function $\varepsilon(\omega)$ contain large uncertainties ($\sim$15% is not uncommon), then they can be multiplied by a factor within this uncertainty so that they reproduce the more precisely known value for ε_0 and n_0^2. The reason to use a renormalizing factor is that this is the simplest operation that can be applied on the data. Thus we assume that the VUV data obtained from the literature do not contain large frequency-dependent systematic errors, since in most studies these errors are not mentioned. On the other hand, reported errors in the determination of the frequencies are generally very small, while reported errors in the absorption strength are larger. However, by comparing data from different sources for the same substance (see below, for example, the case of benzene), one can obtain an estimate for the accuracy of our assumption.

The procedure outlined above is particularly useful for liquids for which we would not expect atomic structure or density related variation in the dielectric data under constant atmospheric conditions. For solids, a natural variation in the dielectric function due to varying structure (grains, defects, etc.) will also lead to a natural variation of n_0^2 and ε_0 [5,6]. In all cases, we only vary the VUV absorption, since IR absorption is usually very small for liquids and known quite accurately. For PTFE, a 15% correction was needed to reproduce the reported value of $\varepsilon_0 = 2.1$. By performing this correction, the obtained value for n_0^2 was 1.77, which compares to reported values in the literature of $n_0^2 \approx 1.74$–1.85 for PTFE surfaces [Fig. 1(a)].

The method described above for creating dielectric functions at imaginary frequencies is far more accurate than creating simple oscillator models using only ε_0 and n_0 and some characteristic UV and IR frequencies of the substances under consideration. The problems with oscillator models become immediately clear when comparing them to real data (Fig. 1). PTFE has at least two major absorption peaks in the UV range, while the simple models would only suggest one peak [7]. The model of Milling $et\ al.$ [1] assumes the peak to be at 5 eV and that of Drummond $et\ al.$ [12] at around 18 eV (compared to 8 and 20 eV as the measurement suggests). The model of [1] completely fails to describe the dielectric data. Although the model of Ref. [12] gives reasonable results, it also fails to describe the dielectric data in the far-UV range.

In order to fit satisfactorily our derived data for $\varepsilon(i\zeta)$, at least five oscillators were necessary. The models of Drummond $et\ al.$ [12] suggest a natural variation in dielectric data for different densities of PTFE. Unfortunately no other dielectric data are available from other sources for PTFE for comparison purposes. However, for polystyrene and silica, multiple sets of data are available. Thus for the solids (except PTFE) we report two sets of data, while for liquids we will report only one. Note that for PTFE, a good approximation of sample dependence or density variation can be obtained by varying the dielectric strength at imaginary frequencies by $\sim$5–10%.

TABLE I. Dielectric data for several substances. n_0 is for the wavelength $\lambda = 589.3$ nm. For solids, the variation of ε_0 and n_0 is shown. For liquids, the mean and standard deviation (as obtained from different sources) are shown at 298 K. Note that for liquids the variation in values is much lower than that of solids. The ε_0 and n_0 values are obtained from Landolt-Bornstein database averages [16]. The oscillator model parameters for the dielectric function at imaginary frequencies, valid in at least the range of 10^{-2}–10^2 eV, are also shown. The first line shows the strength C_i and the second line shows the frequency ω_i (eV). Note that for different substances, a different number of oscillators is used. Furthermore the values of C_i and ω_i are the result from a least-squares fit. They are as such a bit arbitrarily generated and may not correspond to physical frequencies of the molecule. However, the fits always agree well with the fitted data (to within 1%). Numbers in square brackets denote powers of 10.

Material	ε_0	n_0	Oscillator model values
			Low-k solids
PTFE	2.1	1.32–1.36	9.30[−3] 1.83[−2] 1.39[−1] 1.12[−1] 1.95[−1] 4.38[−1] 1.06[−1] 3.86[−2]
			3.00[−4] 7.60[−3] 5.57[−2] 1.26[−1] 6.71[+0] 1.86[+1] 4.21[+1] 7.76[+1]
Silica	3.9–4.1	1.45–1.48	7.84[−1] 2.03[−1] 4.17[−1] 3.93[−1] 5.01[−2] 8.20[−1] 2.17[−1] 5.50[−2]
(set 1)			4.11[−2] 1.12[−1] 1.12[−1] 1.11[−1] 1.45[+1] 1.70[+1] 8.14[+0] 9.16[+1]
Silica	3.9–4.1	1.45–1.48	1.19[+0] 6.98[−2] 1.35[−2] 7.10[−1] 1.80[−1] 5.95[−1] 2.27[−1] 5.58[−2]
(set 2)			5.47[−2] 1.23[−2] 5.74[−4] 1.29[−1] 9.10[+0] 1.43[+1] 2.31[+1] 7.90[+1]
Polystyrene	2.4–2.5	1.55–1.59	1.21[−2] 2.19[−2] 1.79[−2] 3.06[−2] 3.03[−1] 6.23[−1] 3.25[−1] 3.31[−2]
(set 1, 2008)			1.00[−3] 1.32[−2] 3.88[+0] 1.31[−1] 5.99[+0] 1.02[+1] 1.88[+1] 5.15[+1]
Polystyrene	2.4–2.5	1.55–1.59	3.12[−2] 1.17[−2] 2.17[−2] 9.20[−3] 2.93[−1] 6.54[−1] 4.17[−1] 2.13[−2]
(set 2, 1977)			1.18[−1] 9.00[−4] 1.19[−2] 1.56[+0] 6.12[+0] 1.01[+1] 2.02[+1] 6.86[+1]
			Cycloalkanes
Cyclopentane	1.96	1.403	1.51[−2] 1.19[−1] 4.79[−1] 3.00[−1] 5.07[−2]
	( )	( )	2.16[−1] 8.09[+0] 1.07[+1] 1.79[+1] 3.97[+1]
Cyclohexane	2.01	1.424	1.51[−2] 1.34[−1] 5.17[−1] 3.05[−1] 4.65[−2]
	0.02	0.002	2.16[−1] 8.03[+0] 1.09[+1] 1.84[+1] 4.13[+1]
Cycloheptane	2.08	1.44	1.52[−2] 1.50[−1] 5.80[−1] 3.18[−1] 1.81[−2]
	( )	( )	2.18[−1] 8.26[+0] 1.09[+1] 2.04[+1] 6.02[+1]
Cyclooctane	2.12	1.454	1.47[−2] 3.75[−1] 5.45[−1] 1.71[−1] 1.57[−2]
	( )	( )	2.08[−1] 8.67[+0] 1.36[+1] 2.36[+1] 6.61[+1]
			Benzene derivatives
Benzene	2.273	1.498	2.32[−2] 6.99[−3] 8.51[−2] 2.57[−1] 6.59[−1] 2.26[−1] 1.43[−2]
	0.009	4[−4]	8.76[−1] 6.71[+0] 4.48[+0] 1.70[+1] 8.48[+0] 2.33[+1] 7.01[+1]
FluoroBenzene	5.3	1.4629	6.14[−2] 2.38[−2] 4.94[−1] 5.29[−1] 9.63[−2] 1.24[−2]
	0.1	(2[−6])	1.29[−1] 5.52[−2] 7.04[+0] 1.53[+1] 2.68[+1] 8.91[+1]
ChloroBenzene	5.75	1.522	4.92[−2] 2.64[−2] 3.77[−1] 5.89[−1] 3.19[−1] 3.18[−2]
	0.23	0.001	7.89[−2] 1.46[−1] 6.27[+0] 1.16[+1] 2.03[+1] 5.27[+1]
BromoBenzene	5.37	1.558	5.44[−2] 1.84[−2] 4.75[−2] 5.32[−1] 6.45[−1] 2.40[−1] 9.27[−3]
	0.04	0.001	5.02[−3] 3.09[−2] 1.11[−1] 6.75[+0] 1.33[+1] 2.40[+1] 9.99[+1]
IodoBenzene	4.6	1.62	4.08[−3] 7.98[−2] 7.98[−3] 4.20[−1] 7.40[−1] 4.46[−1] 1.26[−2]
	( )	( )	2.60[−2] 9.40[−2] 1.88[+0] 6.37[+0] 1.09[+1] 2.14[+1] 8.86[+1]
Toluene	2.395	1.494	5.61[−3] 6.97[−2] 8.07[−3] 5.15[−1] 5.74[−1] 9.91[−3] 1.18[−1] 1.01[−2]
	0.02	5[−4]	3.40[−2] 9.97[−2] 1.15[+0] 7.23[+0] 1.50[+1] 2.08[+1] 2.59[+1] 7.65[+1]
			Alkanes
Pentane	1.831	1.355	1.91[−2] 1.03[−1] 4.16[−1] 2.39[−1] 5.85[−2]
	0.02	( )	2.38[−1] 7.98[+0] 1.32[+1] 1.79[+1] 3.86[+1]
Hexane	1.887	1.3727	1.86[−2] 1.09[−1] 4.43[−1] 2.82[−1] 3.25[−2]
	0.004	6[−4]	2.31[−1] 7.90[+0] 1.29[+1] 1.93[+1] 4.81[+1]
Heptane	1.914	1.3853	1.89[−2] 1.12[−1] 4.59[−1] 2.89[−1] 3.43[−2]
	0.01	7[−4]	2.31[−1] 7.94[+0] 1.28[+1] 1.92[+1] 4.79[+1]
Octane	1.934	1.3951	1.94[−2] 1.14[−1] 4.72[−1] 2.92[−1] 3.57[−2]
	0.02	4[−4]	2.34[−1] 7.52[+0] 1.30[+1] 1.87[+1] 4.92[+1]
Dodecane	2.014	1.420	1.71[−2] 1.15[−1] 5.66[−1] 2.68[−1] 4.65[−2]
	0.013	0.003	2.17[−1] 7.55[+0] 1.30[+1] 1.90[+1] 4.45[+1]
			Alcohols
Water	78.7	1.3325	1.43[+0] 9.74[+0] 2.16[+0] 5.32[−1] 3.89[−1] 2.65[−1] 1.36[−1]
	0.4	4[−4]	2.29[−2] 8.77[−4] 4.93[−3] 1.03[−1] 9.50[+0] 2.09[+1] 2.64[+1]
Methanol	32.9	1.3266	4.38[−1] 3.24[−1] 1.38[−1] 1.20[−1] 4.45[−1] 2.52[−1] 6.49[−2]
	0.4	4[−4]	6.10[−3] 1.93[−2] 1.02[−1] 4.35[−1] 1.08[+1] 2.01[+1] 3.83[+1]

TABLE I. *(Continued.)*

Material	ε_0	n_0	Oscillator model values
Ethanol	24.8	1.3595	9.57[−1] 1.62[+0] 1.40[−1] 1.26[−1] 4.16[−1] 2.44[−1] 7.10[−2]
	0.4	5[−4]	1.62[−3] 4.32[−3] 1.12[−1] 6.87[+0] 1.52[+1] 1.56[+1] 4.38[+1]
Propanol	20.2	1.3834	4.17[−1] 3.74[−1] 1.87[−1] 1.47[−1] 4.89[−1] 3.06[−1] 1.22[−1]
	0.5	6[−4]	1.97[−4] 7.77[−3] 3.75[−2] 3.41[−1] 1.01[+1] 1.75[+1] 3.17[+1]
Butanol	17.4	1.3974	5.49[−1] 3.14[−1] 1.31[−1] 1.10[−1] 5.44[−1] 2.79[−1] 2.72[−2]
	0.2	6[−4]	2.15[−4] 9.58[−3] 8.26[−2] 5.83[+0] 1.25[+1] 2.04[+1] 6.16[+1]
			Halo-alkanes
Iodomethane	6.89	1.532	1.70[−2] 7.29[−1] 2.63[−1] 2.98[−1] 4.79[−2]
	( )	( )	9.61[−2] 8.01[+0] 1.41[+1] 1.63[+1] 6.76[+1]
Diiodomethane	5.318	1.74	1.94[−2] 9.25[−1] 9.22[−1] 8.59[−2] 9.61[−2]
	0.002	( )	9.38[−2] 7.46[+0] 1.33[+1] 5.85[+1] 1.37[+1]
Tetrachloro-methane	2.216	1.461	1.22[−1] 2.85[−1] 5.63[−1] 2.36[−1] 6.79[−3]
	( )	( )	9.53[−2] 8.42[+0] 1.34[+1] 2.21[+1] 8.74[+1]
			Oily liquids
Glycerol	42.4	1.4697	5.80[−1] 3.23[−1] 2.03[−1] 7.68[−1] 3.70[−1] 2.20[−2]
	1.4	( )	6.94[−3] 3.04[−2] 2.91[−1] 1.07[+1] 2.39[+1] 5.04[+1]
Styrene	2.47	1.544	1.31[−2] 2.30[−2] 3.08[−2] 4.07[−1] 6.04[−1] 3.34[−1] 3.89[−2]
	( )	( )	1.08[−3] 1.50[−2] 1.45[−1] 6.24[+0] 1.15[+1] 1.98[+1] 5.15[+1]

III. CYCLOHEXANE AND BENZENE: APPLICATION OF DIELECTRIC DATA ANALYSIS TO LIQUIDS

The obtained data for liquid cyclohexane (see also the Appendix) [11–15] are shown in Fig. 2. The measured data are taken from the solid state, where the density difference between solid and liquid cyclohexane is about 15% [15]. Since in the VUV domain, atoms act as single absorbers, we can just apply a 15% correction to the data of solid cyclohexane in order to obtain the data for the liquid, while any IR absorption is almost negligible. This is also reflected from the fact that n_0^2 and ε_0 are almost identical ($n_0^2 \approx \varepsilon_0 = 2.02$) [16]. Notably we had to apply an additional 8% correction to the VUV values of the reconstructed liquid data for ε'' in order to reproduce n_0^2 and ε_0 for liquid cyclohexane (which is within the reported experimental accuracy of Ref. [13]).

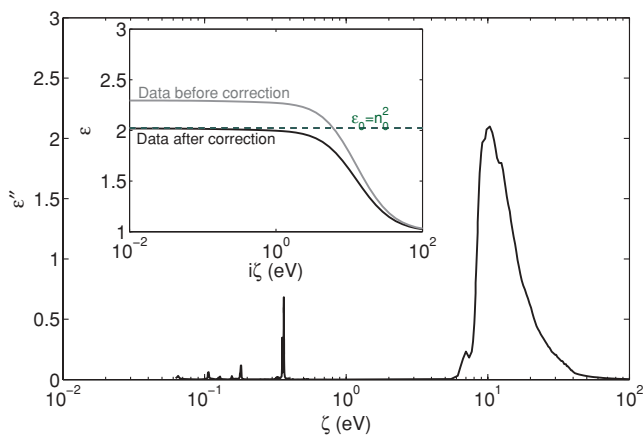For benzene we have two sets of data in the VUV range [13,17] (Fig. 3). Benzene has almost no IR absorption [18], which is reflected by the fact that $n_0^2 \approx \varepsilon_0$. The two different sets of UV data [13,17] lead to quite different dielectric strengths at imaginary frequencies. When performing KK analysis on the data of Ref. [17], we obtained $n_0^2 = 2.09$, while the same procedure with the data of Ref. [13] gave $n_0^2 = 2.53$. This is a difference of 20%, which can lead to very different forces [6]. In Ref. [13] the estimated error is 10%, whereas the data were taken in the solid state suggesting that a correction is needed for the density as well. In Ref. [17] the reported accuracy in the absolute scale is 5%. However, in general, in the chemical literature (as shown in Ref. [17]) a variation of ∼10% for the obtained data is found [17]. Therefore, corrections to the reported values for ε'' and k in Refs. [13] and [17] of 17% and 12%, respectively, were applied for KK consistency with

FIG. 2. (Color online) Dielectric data for cyclohexane. The inset shows dielectric data at imaginary frequencies.
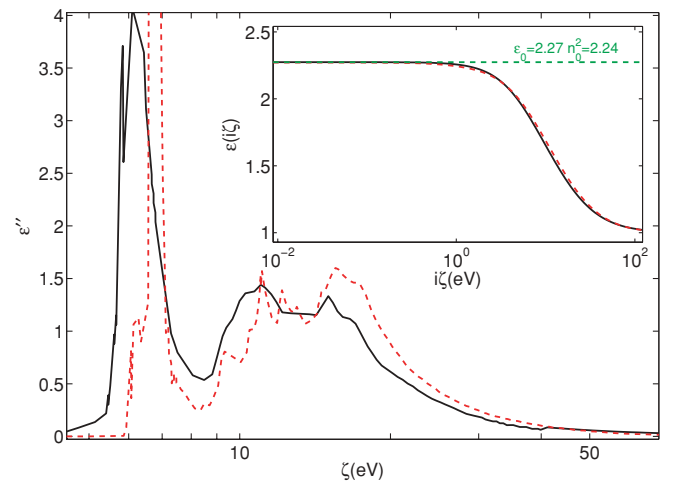

FIG. 3. (Color online) Dielectric data for benzene from different sources. The dashed line was taken from Ref. [17] and solid line from Ref. [13]. The data shown in the graph are already corrected so that they reproduce the correct value for n_0^2.

the known values of $n_0^2 = \varepsilon_0 = 2.244$ [16]. After correcting the data so that they reproduce the correct value of n_0^2 (and ε_0), the difference in dielectric functions at imaginary frequencies for Refs. [13] and [17] is less than 3%, as the inset in Fig. 3 shows.

IV. HALOBENZENES: HOW TO USE SIMILAR MOLECULES IN DIELECTRIC DATA ANALYSIS

For many high-index liquids, the dielectric data over the required frequency range are not available. We will try here to show that when the dielectric function of a very similar molecule is known, then a good estimate of the dielectric function can still be made (similar to the procedure applied for PTFE), and as an example we will apply this procedure to benzene derivatives for which force measurements exist. Note that the dielectric functions for the different benzene derivatives do not differ significantly from each other [Fig. 4(a)] [13]. All benzene derivatives are characterized by a thin absorption peak at $\sim 7\,\mathrm{eV}$ and a broad one at $\sim 20\,\mathrm{eV}$, while they are transparent in the visible range.

We can construct the dielectric function of chlorobenzene at imaginary frequencies using the dielectric data for chlorobenzene [11,13] and measured values for n_0. For comparison purposes, we will also create the dielectric function at imaginary frequencies of chlorobenzene using the dielectric data of pyridine and measured values of n_0 for chlorobenzene. The result of these calculations is shown in Fig. 4(b). The difference is less than 2% for the dielectric function at

imaginary frequencies, suggesting clearly that this method works rather well.

Finally, we have used the VUV chlorobenzene dielectric data to construct the dielectric function of all the halobenzenes. Halobenzenes absorb strongly in the microwave regime for which we have no available dielectric data. Therefore we only used chlorobenzene data in combination with measured values for n_0 for the halobenzenes in applying the KK consistency (Table I). IR absorption data were available for all halobenzenes [19–22] and for toluene [23]. This information was also used for the construction of the dielectric function at imaginary frequencies in the range 10^{-3}–10^2 eV.

V. DIELECTRIC ANALYSIS FOR OTHER LIQUIDS: OSCILLATOR MODEL REPRESENTATIONS

Simple oscillator models (second or third order), which are built with dielectric data in a very limited frequency interval (or a few fixed frequencies), may not be very useful [6]. However, in general, the oscillator representation works well as a parametrization of any dielectric function at imaginary frequencies. We recall that the oscillator model is given by [7]

$$\varepsilon(i\zeta) = 1 + \sum_i \frac{C_i}{1 + (\zeta/\omega_i)^2}. \qquad (2)$$

The coefficient C_i is the oscillator strength at a given (resonance) frequency ω_i. We have fitted these functions to the dielectric functions at imaginary frequencies as obtained with the method described previously. This is done because oscillator functions are convenient to use with Lifshitz theory to calculate the Casimir force. Since in our case they are obtained from measured dielectric data over a wide frequency interval, they should prove quite accurate. Oscillator model representations for many substances, which were constructed as proposed here, are shown in Table I. Finally, the description of how we obtained the dielectric data for the remaining substances [24–40] shown in Table I is described in the Appendix.

For most substances, the valid frequency range of the presented oscillator models is 10^{-2}–10^2 eV, and this is sufficient for finite-temperature force calculations, because the first IR Matsubara term is in this range. For some substances (such as silica and PTFE) the presented oscillator model is valid for any frequency. Recall that for solids we used two sets of dielectric data because of sample dependence [5,6], and for liquids only one because we do not expect any sample dependence.

VI. THEORY CALCULATIONS COMPARED TO FORCE MEASUREMENTS

Measured repulsive Casimir forces have never been compared to Lifshitz theory calculations [41] based on measured dielectric data. Always for one or more substances, simple (sometimes erroneous) second- or third-order oscillator models were used [1–4,6]. We will compare finite-temperature force calculations using Lifshitz theory [41,42], by implementation of the dielectric functions for liquids created with the method presented here, to force measurements [4,42]. All
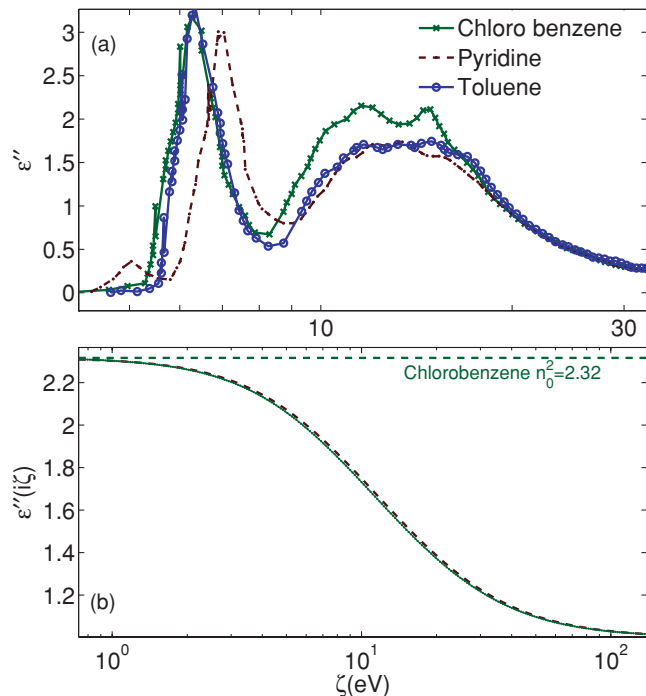

FIG. 4. (Color online) (a) Dielectric functions of several benzene derivatives. (b) The dielectric function of chlorobenzene as constructed from dielectric data of pyridine (dashed line) and chlorobenzene (solid line) normalized using the indicated value of n_0^2.
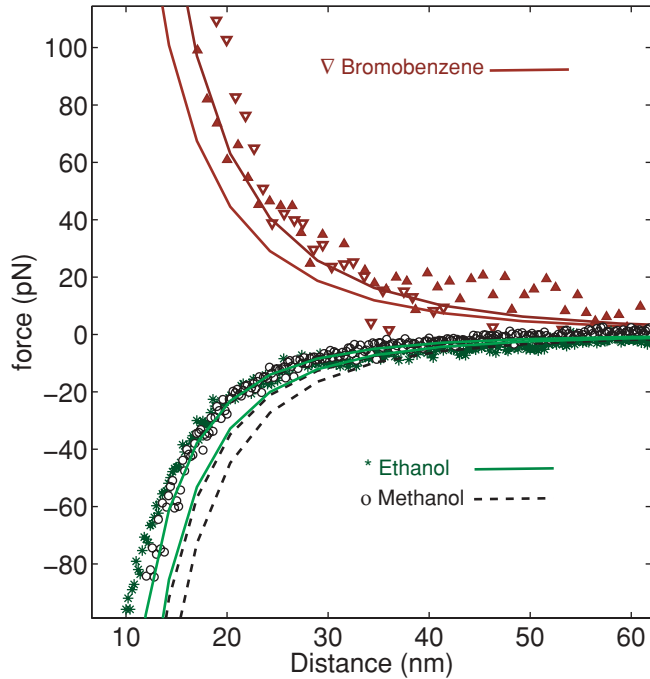
FIG. 5. (Color online) Force measurements between sphere and plate for silica and gold surfaces and the indicated liquids. Dots are experimental data from Refs. [4,43]. The lines represent theory using data from Table I and Ref. [5]. We use two sets of dielectric data for silica. For bromobenzene, the used sphere was 40 μm in diameter, while for ethanol and methanol, a sphere with diameter 18 μm was used. Experimental force data for the bromobenzene system was digitized from a log-log plot [4], thus above 30 nm, not all points are shown.

force measurements were performed between gold and silica surfaces with different liquids [4,43].

For bromobenzene, weak repulsion was measured; while for methanol and ethanol, weak attraction (Fig. 5). The forces obtained with Lifshitz theory using the dielectric data from Table I (for the two sets of silica and the liquids) and the data for gold from Ref. [5] are also shown. A variation of ~30% for the theory is observed due to sample dependence of silica surfaces. The calculations agree at the 30% level with the experiments for all cases. Considering the force variation of 30% due to variation in optical properties of solids and the accuracy issues mentioned in Refs. [6,43], this is a good agreement. Note that the experimental force curves for ethanol and methanol do not appear to differ by ~30% as theory suggests, we attribute this to experimental uncertainty [43].

Note that in Ref. [6] a force variation of 100% was present for the silica-ethanol-gold system, since the reported variation in dielectric data for ethanol [6] was also taken into account. The whole purpose of the work presented here is to deal with such a variation (which we do not expect for liquids). As a result the improvement in theoretical accuracy is roughly a factor of 3 for these systems. Although for PTFE and gold surfaces, almost any liquid leads to repulsion, this is not the case for silica and gold surfaces. Therefore silica provides an excellent test case, and a system for which, using the correct liquid, a sign switch of the force with distance can be expected.

VII. CASIMIR FORCE SIGN SWITCH WITH DISTANCE: IS IT OBSERVABLE?

The smaller the difference between the dielectric function of the liquid and the low-index solid, the larger the uncertainty in force becomes. However, the more likely a sign switch with distance [6]. This is shown in Fig. 6 for silica and gold surfaces and a family of benzene liquids. The calculations were performed with two different sets of dielectric data for silica. For fluorobenzene, the force switches sign at 25 nm for one silica sample or it is attractive for the other silica sample. For benzene, it switches sign at 3 nm or it is attractive with unusual force scaling at 50 nm. For chlorobenzene, it switches sign at 3 nm or it is repulsive. Note that either the force switches sign at extremely small distances, or when it switches sign at larger distances it is very weak. Therefore a very sensitive force measurement device is needed for the detection of the sign switch.

We obtained similar results for PTFE and gold, in combination with low-absorption liquids such as water, methanol, and pentane. In this case, the force switches sign, being attractive below 10 nm. For ethanol, we obtained repulsion (two times weaker than for cyclohexane). Therefore our results are also in agreement with those presented in Ref. [3]. For all other liquids, the force was repulsive in the case of PTFE and gold surfaces. For a slightly higher density PTFE sample, short-range attraction may be observed for more liquids. For a
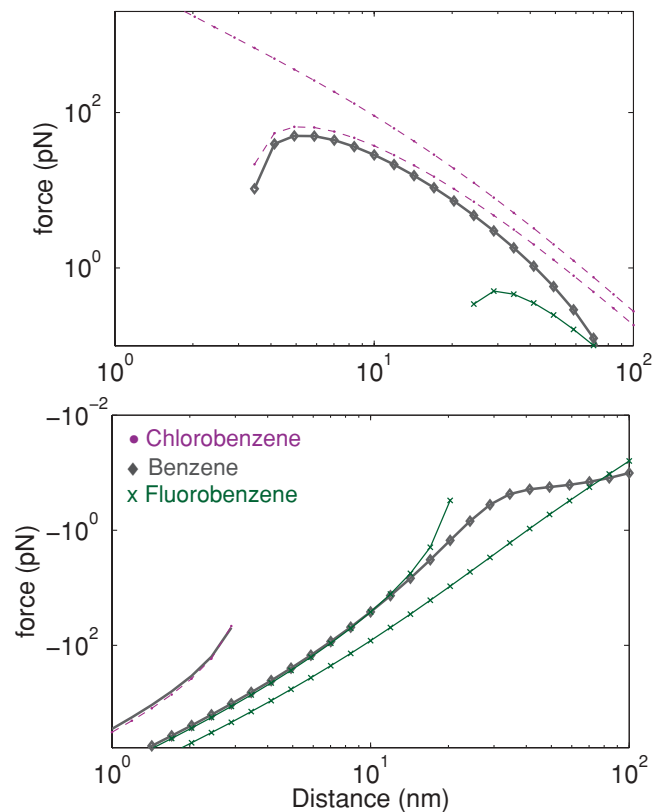

FIG. 6. (Color online) Casimir forces between a silica sphere (diameter 18 μm) and a gold surface immersed in various liquids as indicated. The force calculations were performed for two dielectric data sets for silica. Plots are shown for repulsive (upper part) and attractive (lower part) forces.

slightly lower density PTFE sample, even for water, one may obtain divergent repulsion. However, we would like to note that water is notorious for capillary stiction, even in liquid environments [3,44].

VIII. THE CASE OF CASIMIR REPULSION

There are not many combinations of materials for which Casimir repulsion is obtained. There are even less combinations for which this repulsion is strong. PTFE is the material of choice if we want to obtain strong Casimir repulsion, because it has the smallest dielectric strength of any material. Stronger Casimir repulsion would be easier to measure, and the theoretical uncertainty would also be smaller since the dielectric contrast is larger [6]. Force calculations with some high-index liquids between gold and PTFE are shown in Fig. 7. Compared to cyclohexane, using benzene and bromobenzene already yields 3–4 times stronger repulsion, while di-iodomethane gives even 10 times stronger repulsion. Since the latter liquid has one of the highest refractive indices of any pure liquid, much stronger repulsion will be very hard to obtain. For example, liquids with refractive index $n_0 > 1.74$ have very undesirable other properties and are often based on solutions with (highly toxic) solid components. In any case, Fig. 7 thus shows that when using real liquids, Casimir repulsion can be varied within a factor roughly of 10 with a typical PTFE surface. Note that when using silica instead of PTFE, repulsion will be much weaker, or attractive. Thus it should be possible to increase the repulsive force by a factor 5–10, compared to what has been measured to date [1–4]. Finally, note that van der Waals or Casimir repulsion in liquids is stable with respect to perturbations, it exists between macroscopic objects, and it does not require a dedicated geometry as is required for obtaining repulsion in air or a vacuum [45].
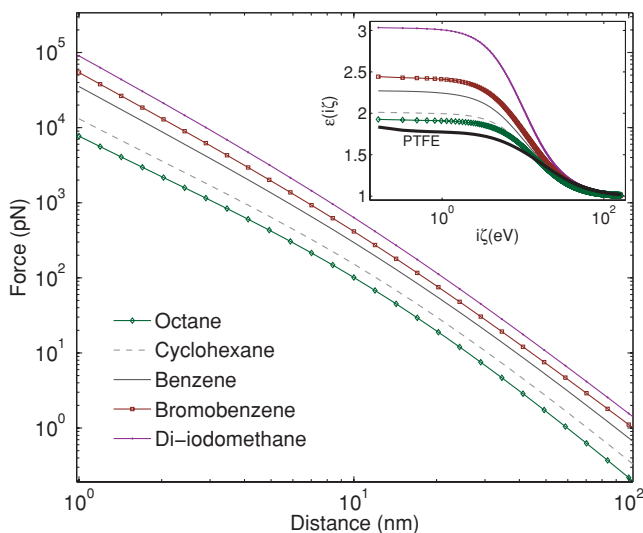
IX. CONCLUSIONS

We have presented here measured dielectric data obtained from the literature for PTFE, polystyrene, silica, and more than 20 liquids. A scheme was provided to deal with the variation in dielectric data for liquids, which leads to high uncertainty in the Casimir-Lifshitz force calculation. Using this scheme, we have created dielectric data at imaginary frequencies for liquids, and we provided arguments why these data should be accurate to within a few percent error. Consequently, we were able to provide more accurate force calculations for systems immersed in liquids. These force calculations with the new data are in good agreement with recent measurements in bromobenzene and alcohols. Besides cyclohexane, we have suggested liquids for which much stronger Casimir repulsion exists. Dielectric data for simple oils were presented, and they can be very useful for ultra-low-friction lubrication [3] using repulsive Casimir forces.

Force calculations with the new data suggest that a sign switch with distance will be very hard to measure due to the extremely small forces involved. Because of sample variation of solids, it is suggested that a "family" of similar liquids is required for the detection of this phenomenon, or the dielectric function of the solid should be accurately measured and an appropriate liquid is chosen. The dielectric data provided here should also be very useful for accurate prediction of contact angles [46] and more precise calculations for quantum torques [47].

APPENDIX

PTFE dielectric data. The dielectric data in the x-ray region >30 eV can be modeled as in [8]. The vacuum UV data in the range of 5–25 eV are taken from a molecule very similar to PTFE [poly(hexafluoro-1,3-butadiene)] [9]. In the visible and near IR, Teflon is transparent and as a result absorption is negligible in this range. IR and THz data were taken from Refs. [10] and [11].

Polystyrene and silica. Two sets of data for silica were obtained from Ref. [24]. For polystyrene, THz and IR data were obtained from Refs. [25,26], and the two different sets of UV data were obtained from Refs. [27,28].

(Cyclo)alkanes. The procedure for liquid cyclohexane is as follows. Dielectric data for the x-ray range >40 eV are modeled [8]. Data in the range 10–40 eV are taken from Ref. [13]. The IR range data are taken from [14]. Particularly the errors in the VUV data of Ref. [13] are $\pm10\%$. These data are the most important for the construction of the dielectric function at imaginary frequencies.

The dielectric function of the other cycloalkanes were all constructed from the data for cyclohexane and corrected to reproduce the corresponding n_0^2 and ε_0 values for a specific

FIG. 7. (Color online) Casimir forces between PTFE and gold surfaces between a sphere (diameter 18 μm) and a plate immersed in various high-index liquids. The inset shows dielectric data for PTFE and the liquids.

cycloalkane [16,29]. For the simple alkanes, UV data in the range 7–200 eV were taken from Ref. [30]. The IR or THz absorption was almost negligible for all (cyclo)alkanes, reflected by the fact that $n_0^2 \approx \varepsilon_0$ within the error bars [16]. The dielectric function for dodecane was estimated from n_0^2 and ε_0 and dielectric data of octane.

Water and alcohols. The dielectric data for water were obtained from Segelstein [31]. These data produce a too high value for n_0^2. Therefore, we applied a 15% correction to the absorption in the UV range (>5 eV). While there are many other studies for water, we do not wish to provide a review for water here, and we use only the data of Segelstein. Note that Segelstein's data [31] for k is also not perfectly KK consistent for n, as it differs by 15%. For the alcohols, UV data were obtained from [6,8,32–35], and IR and THz from [36,37]; again, the UV data were made consistent with measured values for n_0^2 [16].

Halo-alkanes. For methyl iodide dielectric data in the UV range 4–500 eV were found in [38], and IR data in the range 0.05–0.5 eV in [39]. A very similar liquid, methyl diiodide, has one of the highest refractive indices ($n_0 = 1.74$) of any pure liquid while being not very toxic but slightly unstable under light. The dielectric function of methyl diiodide was constructed using the IR data [39], and methyl iodide UV data [38]. The UV data were corrected with a factor to reproduce $n_0 = 1.74$. For tetrachloromethane, data in the IR (0.02–0.5 eV) and UV (5–200 eV) ranges were obtained from Refs. [22,40].

The magnitude of the VUV absorption [40] was varied 15% to reproduce ε_0. This resulted in a value for $n_0 = 1.449$ as compared to the reported value of 1.461 [16].

Viscous or oily liquids. Finally we present data for simple, highly viscous or oily liquids. These liquids are very interesting, since besides lubrication, repulsive Casimir forces will result in even lower or negligible friction with some substances [3]. One of these liquids is styrene. It is the building block of polystyrene and has a high refractive index. We have used the dielectric data of polystyrene and constructed the dielectric function of styrene to properly reproduce n_0 and ε_0. Repulsive forces even result for the silica-styrene-metal system. Thus styrene is extremely interesting for systems in which glass and metal parts come into contact, which is not uncommon in micro- or nano-mechanical devices. While it is not as strongly absorbing as styrene, glycerol has a relatively high refractive index and is often used in colloid physics. Compared to the simple alcohols, glycerol ($C_3H_8O_3$) is structurally most similar to methanol (CH_4O). It also has a high value for ε_0 like methanol. Therefore, we will use the data of methanol and multiply the VUV data with a factor to reproduce $n_0 = 1.4697$ for glycerol. For all simple alcohols, the structure of the UV peaks does not change significantly apart from a factor, and IR absorption for liquids is weak. As a result, we expect the force calculations, based on the constructed dielectric function at imaginary frequencies, to be quite precise, as they are for all the other liquids.

[1] A. Milling, P. Mulvaney, and I. Larson, J. Colloid Interface Sci. **180**, 460 (1996).

[2] S. Lee and W. M. Sigmund, J. Colloid Interface Sci. **243**, 365 (2001).

[3] A. A. Feiler, L. Bergstrom, and M. W. Rutland, Langmuir **24** (6), 2274 (2008).

[4] J. N. Munday, F. Capasso, and V. A. Parsegian, Nature (London) **457**, 170 (2009).

[5] V. B. Svetovoy, P. J. van Zwol, G. Palasantzas, and J. T. M. De Hosson, Phys. Rev. B **77**, 035439 (2008).

[6] P. J. van Zwol, G. Palasantzas, and J. T. M. De Hosson, Phys. Rev. B **79**, 195428 (2009).

[7] D. B. Hough and L. R. White, Adv. Colloid Interface Sci. **14**, 3 (1980).

[8] B. L. Henke, E. M. Gullikson, and J. C. Davis, At. Data Nucl. Data Tables **54**, 181 (1993).

[9] K. Seki *et al.*, Mol. Cryst. Liq. Cryst. **355**, 247 (2001).

[10] E.-H. Korte and A. Röseler, J. Mol. Struct. **661**, 579 (2003).

[11] M. Naftaly and R. E. Miles, in *Terahertz Frequency Detection and Identification of Materials and Objects*, edited by R. E. Miles *et al.* (Springer, Dordrecht, Netherlands, 2007), pp. 107–122.

[12] C. J. Drummond, G. Georgaklis, and D. Y. C. Chan, Langmuir **12**, 2617 (1996).

[13] U. Killat, Phys. C: Solid State Phys. **7**, 2396 (1974).

[14] C. D. Keefe and J. E. Pickup, Spectrochim. Acta, Part A **72**, 947 (2009).

[15] H. Chew and R. Chan, Can. J. Chem. **51**, 2141 (1973).

[16] The Landolt Börnstein Database (Springer) [http://www.springermaterials.com].

[17] R. Feng, G. Cooper, and C. E. Brion, J. Electron Spectrosc. Relat. Phenom. **123**, 199 (2002).

[18] J. E. Bertie and C. D. Keefe, J. Mol. Struct. **695**, 39 (2004).

[19] C. D. Keefe, J. Barrett, and L. L. Jessome, J. Mol. Struct. **734**, 67 (2005).

[20] J. E. Bertie, R. N. Jones, and Y. Apelblat, Appl. Spectrosc. **48**, 144 (1994).

[21] C. D. Keefe, L. A. Donovan, and S. D. Fleet, J. Phys. Chem. A **103**, 6420 (1999).

[22] T. G. Goplen, D. G. Cameron, and R. N. Jones, Appl. Spectrosc. **34**, 657 (1980).

[23] J. E. Bertie *et al.*, Appl. Spectrosc. **48**, 127 (1994).

[24] R. Kitamura, L. Pilon, and M. Jonasz, Appl. Optics **46**, 8118 (2007).

[25] U. Strom *et al.*, Solid State Commun. **15**, 1871 (1974).

[26] W. R. Folks *et al.*, Int. J. Infrared Millim. Waves **27**, 1553 (2006).

[27] T. Inagaki *et al.*, Phys. Rev. B **15**, 3243 (1977).

[28] R. H. French *et al.*, Aust. J. Chem. **60**, 251 (2007).

[29] R. H. Stokes, J. Chem. Thermodyn. **5**, 379 (1973).

[30] J. W. Au *et al.*, Chem. Phys. **173**, 209 (1993).

[31] D. J. Segelstein, Ph.D. thesis, University of Missouri, Kansas City, 1981.

[32] R. Feng and C. E. Brion, Chem. Phys. **282**, 419 (2002).

[33] M. Ogawa and G. R. Cook, J. Chem. Phys. **28**, 747 (1957).

[34] D. R. Salahub and C. Sandorfy, Chem. Phys. Lett. **8**, 71 (1971).

[35] H. Koizumi *et al.*, J. Chem. Phys. **85**, 4276 (1986).

[36] P. P. Sethna and D. J. Williams, Phys. Chem. **83**, 405 (1979).

[37] J. E. Bertie *et al.*, Vib. Spectrosc. **8**, 215 (1995).

[38] T. N. Olney, G. Cooper, and C. E. Brion, Chem. Phys. **232**, 211 (1998).

[39] F. L. Voelz *et al.*, J. Opt. Soc. Am. **43**, 1061 (1953).

[40] G. R. Burton *et al.*, Chem. Phys. **181**, 147 (1994).

[41] I. M. Dzyaloshinskii, E. E. Lifshitz, and L. Pitaevskii, Sov. Phys. Usp. **4**, 153 (1961).

[42] J. N. Munday, F. Capasso, V. A. Parsegian, and S. M. Bezrukov, Phys. Rev. A **78**, 032109 (2008).

[43] P. J. van Zwol, G. Palasantzas, and J. Th. M. De Hosson, Phys. Rev. E **79**, 041605 (2009).

[44] J. W. G. Tyrrell and P. Attard, Phys. Rev. Lett. **87**, 176104 (2001).

[45] M. Levin *et al.*, e-print arXiv:1003.3487.

[46] C. J. Drummond and D. Y. C. Chan, Langmuir **13**, 3890 (1997).

[47] J. N. Munday, D. Iannuzzi, Y. Barash, and F. Capasso, Phys. Rev. A **71**, 042102 (2005).